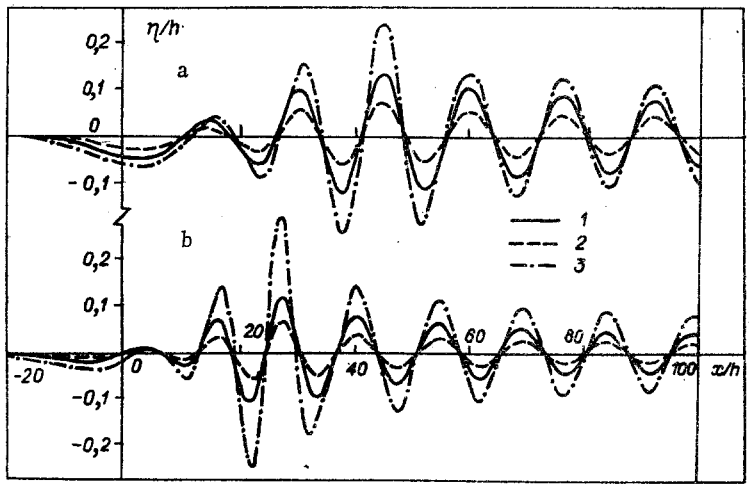

Fig. 5

$$\frac{k}{(1+\varepsilon)\,\mathrm{th}\,kH_1+\mathrm{th}\,kH_2}<\frac{\Lambda\varepsilon}{(1+\varepsilon)\,[V\sin(\theta+\alpha)-\sin\theta]^2}.$$

The wave motion obtained for the stationary problem examined above will always be stable.

LITERATURE CITED

1. L. N. Sretenskii, Theory of Wave Motions of Fluids [in Russian], Nauka, Moscow (1977).
2. I. N. Kochina, "On waves on the interfacial surface of two fluids flowing at an angle to each other," Prikl. Mat. Mekh., 19, No. 5 (1955).
3. L. S. Gandin, "On wave stability at the interfacial surface of streams directed at an angle to each other," Izv. Akad. Nauk SSSR, Ser. Geofiz., No. 3 (1957).
4. J. W. Miles, "Internal waves generated by a horizontally moving source," Geophys. Fluid Dynam., 2, 1 (1971).

APPARENT INTERNAL WAVES IN A FLUID WITH EXPONENTIAL DENSITY DISTRIBUTION

S. A. Makarov and Yu. D. Chashechkin

UDC 532.593

On the basis of a modified stationary phase method proposed in [1, 2], the constant phase surfaces of internal waves excited by a body moving at an arbitrary angle to the horizon, which agree satisfactorily with those observed experimentally, are determined in [3] in the plane and three-dimensional cases. Taking account of the integral transforms [4, 5], the plane and spatial problems of wave motions occurring during the flow around submerged sources and sinks of identical intensity by a uniform fluid stream stratified with respect to the density are considered by numerical methods in a linear formulation in [6]. The asymptotic solution for the wave field excited by a dipole and an arbitrary source-sink system moving in an exponentially stratified fluid is obtained in [7, 8]. These solutions describe the wave pattern occurring during motion of a body at high velocities.

The purpose of this paper is the determination of the amplitude phase characteristics of apparent internal waves in a fluid with an exponential density distribution for uniform horizontal body displacement in a broad range of motion regimes (including motion at low velocities) and their subsequent comparison with the results of laboratory experiments. Dissipative and diffusion effects (i.e., the change in particle density during motion is not

Moscow. Translated from Zhurnal Prikladnoi Mekhaniki i Tekhnicheskoi Fiziki, No. 6, pp. 47-54, November-December, 1981. Original article submitted October 13, 1980.

 0021-8944/81/2206-0772$07.50

taken into account) and the influence of the free surface are neglected in the solution. It is considered that the fluid is infinitely deep.

The system of hydrodynamic equations governing the velocity field $\mathbf{v}$ has the form

$$(\partial/\partial t + \mathbf{v}\nabla)\rho\mathbf{v} = -\nabla p + \rho\mathbf{g},\ (\partial/\partial t + \mathbf{v}\nabla)\rho = 0,\ \nabla\mathbf{v} = m, \tag{1}$$

where t is the time, ρ is the density, p is the pressure, g is the acceleration of gravity, m(x, y, z, t) is the source and sink distribution in the fluid, and $\nabla = \mathbf{l}\partial/\partial x + \mathbf{m}\partial/\partial y + \mathbf{n}\partial/\partial z$.

The analysis is performed in the OXYZ laboratory coordinate system (the X axis is directed along the line of body motion, the Z axis is vertically upward) and the coordinate system OX*YZ ($x^* = x - Ut$) coupled to the body.

The problem is solved in the Boussinesq approximation. The dimensional parameters of the problem are: $\rho_0(z) = \rho_0(0)\exp[-z/\Lambda]$ is the fluid density, $\Lambda = [d\ \ln\rho_0(z)/dz]^{-1}$ is the scale of the stratification, T is the period and the frequency of free internal vibrations in the fluid is $N = \sqrt{g/\Lambda}$, $T = 2\pi/N$; d is the vertical and L the horizontal dimension of the body, and U is the velocity of its motion; η_0 is the amplitude and A the phase of the internal wave.

The nondimensional parameters are: $Fr = U^2/N^2d^2$ is the internal Froude number; $C = \Lambda/d$ is the scale ratio; $\Psi = L/d$ is the body elongation; $x^\circ = x^*N/AU$, $y^\circ = yN/AU$, $z^\circ = zN/AU$ are dimensionless coordinates.

Irrotational flow around a body by a stream of homogeneous ideal fluid is equivalent to the flow around a combination of sources and sinks [9]. This result can be extended to a stratified fluid also in the case of small gradients, when the fluid density varies insignificantly in ranges on the order of the body dimension [6].

Motion of a dipole and a system consisting of a source and sink of equal intensity located at a range $2a$ is considered.

Taking account of the coupling between the vertical deviation of a constant density surface from the equilibrium position $\eta(x, y, z, t)$ and the vertical velocity component [7], the linearized system (1) is reduced to the following equation:

$$\left\{\frac{\partial^2}{\partial t^2}\left(\frac{\partial^2}{\partial x^2}+\frac{\partial^2}{\partial y^2}+\frac{\partial^2}{\partial z^2}\right)+N^2\left(\frac{\partial^2}{\partial x^2}+\frac{\partial^2}{\partial y^2}\right)\right\}[\rho_0(z)\,\eta(x,y,z,t)] = \frac{\partial}{\partial t}\frac{\partial}{\partial z}[\rho_0(z)\,m(x,y,z,t)]. \tag{2}$$

Values of m(x, y, z, t) are presented in [6, 7] for the motion of plane and three-dimensional bodies.

A solution of (2) is sought with zero boundary conditions at infinity. Steady-state wave motion is considered.

The internal waves being formed during uniform body motion in a stratified fluid are called apparent since the wave pattern is stationary in the coordinate system coupled to the body.

Taking into account that $\omega = -\alpha U$ for uniform horizontal body motion, the asymptotic solution of (2) has the form [1]

$$\eta(x^*, y, z) = \frac{4\pi^2}{r^*}\sum\frac{BF(\alpha,\beta,\gamma)\exp[i(\alpha x^*+\beta y+\gamma z)]}{|\nabla_k G|\sqrt{|K|}}+O\left(\frac{1}{r^{*2}}\right) \tag{3}$$

as $r^*\to\infty$ along any radius-vector $\mathbf{q}$; the summation is over all points $\mathbf{k} = \{\alpha, \beta, \gamma\}$ of the wave number surface defined by the dispersion relation

$$G(\alpha, \beta, \gamma) = (\alpha U)^2(\alpha^2 + \beta^2 + \gamma^2) - N^2(\alpha^2 + \beta^2) = 0. \tag{4}$$

in which the normal to the surface is parallel to $\mathbf{q}$ and

$$\frac{\mathbf{r}^*\cdot\nabla_k G}{\dfrac{\partial G}{\partial\omega}} > 0\left(\nabla_k = \mathbf{l}\frac{\partial}{\partial\alpha} + \mathbf{m}\frac{\partial}{\partial\beta} + \mathbf{n}\frac{\partial}{\partial\gamma}\right) \tag{5}$$

under the condition that the surface (4) has nonzero Gaussian curvature K at each of these points [1]. The coefficient B depends on the sign of the curvature and the shape of the wave number surface (4), while $F(\alpha, \beta, \gamma)$ is the Fourier transform of the right side of (2).

By analogy with [1], the asymptotic solution of (2) in the plane case (the coordinates {x, z}) is

$$\eta(x^*, z) = \sqrt{\frac{8\pi^3}{r^*}} \sum \frac{Bf(\alpha, \gamma) \exp\left[i\left(\alpha x^* + \gamma z^* + \frac{\pi}{4}\operatorname{sgn} K\right)\right]}{|\nabla_k G| \sqrt{|K|}} + O\left(\frac{1}{r^*}\right) \tag{6}$$

as $r^* \to \infty$ along any radius vector $\mathbf{q}$: summation is over all points $\mathbf{k} = \{\alpha, \gamma\}$ of the curve

$$G(\alpha, \gamma) = (\alpha U)^2(\alpha^2 + \gamma^2) - N^2\alpha^2 = 0,$$

where the normal to the curve is parallel to $\mathbf{q}$ and (5) is satisfied.

As is seen from (3) and (6), the constant-phase surfaces have the form $\mathbf{k}\cdot\mathbf{r}^* = A$. Since the vector $\mathbf{r}^*$ is parallel to the normal to the surface $G = 0$ at the point $\mathbf{k}$, then

$$\mathbf{r}^* = \frac{A}{\mathbf{k}\cdot\nabla_k G} \nabla_k G. \tag{7}$$

Taking account of (4), it follows from the solution of the system (7) that the constant-phase surfaces are described in the three-dimensional case by the equation

$$(x^0)^2 = [(y^0)^2 + (z^0)^2]\left[\frac{1}{(z^0)^2} - 1\right], \tag{8}$$

which agrees with [3, 10]. In the plane case

$$(x^0)^2 + (z^0)^2 = 1. \tag{9}$$

Formulas (8) and (9) have been derived for a point source, when no interference occurs between the waves excited by its distinct parts, which could alter the pattern obtained for the constant-phase surfaces.

The inequality (5) is the radiation condition according to which all the waves are generated by a source and do not arrive at infinity. It follows therefrom that wave-formation occurs only behind the moving body, i.e., for $x^* < 0$, and in the spherical $\{r^*, \varphi, \theta\}$ coordinates coupled to the body $x^* = r^* \cos\theta$, $y = r^* \sin\theta \cos\varphi$, $z = r^* \sin\theta \sin\varphi$ for $\theta > \pi/2$.

The points $\mathbf{k} = \{\alpha, \beta, \gamma\}$ of the wave number surface (4), in which the normal to the surface is in agreement with the direction chosen $\mathbf{r}^* = (x^*, y, z)$, are found from the system

$$(\alpha U)^2(\alpha^2 + \beta^2 + \gamma^2) - N^2(\alpha^2 + \beta^2) = 0, \quad [\nabla_k G \cdot \mathbf{r}^*] = 0. \tag{10}$$

The vector equation of the system (10) contains two linearly independent equations. Taking account of the α, β, and γ determined from (10):

$$\alpha = \pm\frac{N}{U}\sin\varphi\cos\theta, \quad \beta = \pm\frac{N}{U}\frac{\cos^2\theta}{\sin\theta}\sin\varphi\cos\varphi, \quad \gamma = \pm\frac{N}{U}\frac{1-\cos^2\theta\sin^2\varphi}{\sin\theta}$$

the wavelength is

$$\lambda = \frac{2\pi}{\sqrt{\alpha^2+\beta^2+\gamma^2}} = \frac{UT}{\sqrt{1+\frac{x^{*2}y^2}{(y^2+z^2)^2}}} = \frac{UT\sin\theta}{\sqrt{1-\sin^2\varphi\cos^2\theta}}. \tag{11}$$

The wavelength in the $y = 0$ plane is identical everywhere and equals $\lambda_0 = UT$; outside this plane λ tends to zero as it approaches the X axis.

In the case of uniform horizontal motion of a dipole in a deep fluid with weak stratification, the vertical displacement η defined by (3) agrees with the solution in [7]. For small U (or large k), a singularity of the form $1/U$ is observed in the solution in [7].

In the case of motion of a source–sink system, it follows from (3) that

$$\eta_1(r^*, \theta, \varphi) = \frac{R^2}{r^*}\frac{\sqrt{a^2+R^2}}{a}\frac{\sqrt{1-\sin^2\varphi\cos^2\theta}}{\sin\theta}, \tag{12}$$
$$\sin\left(\frac{Na}{U}\sin\varphi\cos\theta\right)\cos\left(\frac{Nr^*}{U}\sin\varphi\right) + O\left(\frac{1}{r^{*2}}\right),$$
$$r^* \to \infty, \ \pi/2 < \theta < \pi \ \ (\text{for} \ \ \theta = \pi, \ K = 0).$$

The vertical displacement (12) does not vanish as U→0. Upon going over to the laboratory coordinate system $\eta_1(x, y, z, t)$ does not tend to zero at the fixed point x, y, z ($y \neq 0$) as $t \to \infty$ exactly as the solution in [7].

In the plane case for flow around a dipole, it follows from (6) that

$$\eta_2(x^*, z) \sim \sqrt{\frac{2\pi}{r^*}} R^2 \frac{z}{r^*} \sqrt{\frac{N}{U}} \cos\left(\frac{Nr^*}{U} - \frac{\pi}{4}\right) + O\left(\frac{1}{r^*}\right), \tag{13}$$

$$r^* \to \infty, \; x^* < 0,$$

and for the flow around a source–sink system

$$\eta_3(x^*, z) \sim \sqrt{\frac{2\pi}{r^*}} \frac{R}{\operatorname{arctg}\left(\frac{a}{R}\right)} \frac{z}{x^*} \sqrt{\frac{U}{N}} \sin\left(\frac{Na}{U} \frac{x^*}{r^*}\right) \cos\left(\frac{Nr^*}{U} - \frac{\pi}{4}\right) + O\left(\frac{1}{r^*}\right), \tag{14}$$

$$r^* \to \infty, \; x^* < 0.$$

Both $\eta_2(x, z, t)$ and $\eta_3(x, z, t)$ tend to zero as $t \to \infty$; however, only (14) vanishes as U→0.

The singularities noted above for the solutions for point perturbations, the dipole in [7], the source–sink pair (12), indicate the nonequivalence of replacing the motion of a three-dimensional body in an inviscid fluid by the motion of point perturbations for not only low [7] but even high velocities when $Fr \gg 1$ and can be eliminated by replacing the delta function in the system (1) by a sequence of classical functions of the form

$$\frac{\exp[-r^2/l^2]}{(l\sqrt{\pi})^3} \to \delta(\mathbf{r}), \quad l \to 0. \tag{15}$$

The case under consideration of the flow around distributed sources and sinks at ranges $bl < r \ll \Lambda$ ($b \gg 1$) is equivalent to the flow around point sources and sinks of intensity $M_1 = M_0 \operatorname{erf}^3(b)$, which corresponds to the flow around an ovoid, where M_0 is the intensity of the point sources [9].

Then taking account of (5) it follows from (3) that in the Boussinesq approximation ($\lambda_0 = UT \ll \Lambda$)

$$\eta^+(r^*, \theta, \varphi) \sim \exp\left[\frac{l^2}{4\Lambda^2}\right] \exp\left[-\left(\frac{\pi l}{\lambda}\right)^2\right] \frac{R^2}{r^*} \frac{\sqrt{a^2 + R^2}}{a} \frac{\sqrt{1 - \sin^2\varphi\cos^2\theta}}{\sin\theta} \tag{16}$$

$$\times \sin\left(\frac{Na}{U}\sin\varphi\cos\theta\right) \cos\left(\frac{Nr^*}{U}\sin\varphi + \operatorname{sgn}(\sin\varphi)\frac{l^2 N}{2\Lambda U}\frac{1 - \sin^2\varphi\cos^2\theta}{\sin\theta}\right)$$

$$+ O\left(\frac{1}{r^{*2}}\right), \quad r^* \to \infty, \quad \frac{\pi}{2} < \theta < \pi.$$

The second exponential factor results in the rapid attenuation of (16) as U→0 and exerts slight influence for high U. For high velocities $\eta^+ \sim 1/U$, the amplitude $|\eta_0^+|$ of the vertical displacement (16) has maximums at the points U_n determined for $l \ll \lambda_0/\pi$ from the condition

$$\frac{Na}{U_n}|\sin\varphi\cos\theta| = \frac{\pi}{2} + \pi n, \quad n = 0, 1, 2, \ldots \tag{17}$$

as the velocity diminishes.

As l increases, the maximums of the amplitudes shift negligibly toward higher U.

The dependence of the internal wave amplitude on the streamlining velocity for small U such that $Fr_a = U^2/(N^2a^2) < 1$ is explained by interference of waves from coherent sources (sources and sinks) located at the range $2a$. The maxima of the amplitudes are observed in the XZ plane for $U = U_n$ determined from

$$\frac{Na}{U_n}|\cos\theta| = \frac{\pi}{2}(2n + 1), \quad n = 0, 1, 2, \ldots, \tag{18}$$

from which it follows that

$$2a|\cos\theta| = n\lambda_n + \lambda_n/2, \; \lambda_n = U_n T,$$

which is a condition of the interference. The appearance of the $\lambda_n/2$ is related to the opposing effects of the source and sink.

It follows from (18) that for low velocities ($Fr_a < 1$), there are several amplitude maxima at different angles θ_n

$$|\cos\theta_n| = \frac{U}{Na}\frac{\pi}{2}(2n+1), \quad n = 0, 1, 2, \ldots \tag{19}$$

As the velocity increases, the maxima shift to the trace axis.

For the motion of an extended body with elongation $\xi = a/R$ the internal wave amplitude is $|\eta_0^+| \sim \sqrt{1+\xi^2}$ for $Fr_a \gg 1$, which agrees with [6], while $|\eta_0^+| \sim \sqrt{1+1/\xi^2}$ for $Fr_a < 1$ and decreases as the elongation grows.

The shape of the constant-wave surface differs somewhat from (8) for motion of the distributed source–sink since the phase addition

$$\operatorname{sgn}(\sin\varphi)\frac{l^2N}{2\Lambda U}\frac{1-\sin^2\varphi\cos^2\theta}{\sin\theta},$$

whose value increases with the approach to the X axis, enters into (16).

Upon going over to the laboratory coordinate system OXYZ, it follows from (16) that

$$\begin{aligned}\eta^+(O, y, z, t) = &-\exp\left[\frac{l^2}{4\Lambda^2}\right]\exp\left[-\frac{N^2l^2}{4U^2}\left(1+\frac{(Ut)^2y^2}{(y^2+z^2)^2}\right)\right] \\ &\times\frac{\sqrt{a^2+R^2}}{a}\frac{R^2}{\sqrt{y^2+z^2}}\sqrt{1-\frac{z^2}{y^2+z^2}\frac{(Ut)^2}{(Ut)^2+y^2+z^2}} \\ &\times\sin\left(\frac{Na}{U}\frac{z}{\sqrt{y^2+z^2}}\frac{Ut}{\sqrt{(Ut)^2+y^2+z^2}}\right)\cos\left\{\frac{N}{U}\sqrt{(Ut)^2+y^2+z^2}\right. \\ &\left.\times\left[\frac{z}{\sqrt{y^2+z^2}}+\frac{l^2}{2\Lambda}\frac{\operatorname{sgn}(z)}{\sqrt{y^2+z^2}}\left(1-\frac{z^2}{y^2+z^2}\frac{(Ut)^2}{(Ut)^2+y^2+z^2}\right)\right]\right\} \\ &+O\left(\frac{1}{(Ut)^2+y^2+z^2}\right), \quad \sqrt{(Ut)^2+y^2+z^2}\to\infty, \quad t>0.\end{aligned} \tag{20}$$

The expression (20) vanishes as $t\to\infty$ for $y = 0$ because the term $\sqrt{1-\frac{z^2}{y^2+z^2}\frac{(Ut)^2}{(Ut)^2+y^2+z^2}}$ decreases, and for $y \neq 0$ because of the decrease in the second exponential factor. The frequency of oscillation tends to

$$\frac{N}{\sqrt{y^2+z^2}}\left[z+\frac{l^2}{2\Lambda}\frac{y^2}{y^2+z^2}\right] \simeq N\frac{z}{\sqrt{y^2+z^2}}$$

as time passes.

The first oscillations have a period somewhat greater than $T(\sqrt{y^2+z^2})/z$.

The asymptotic solution is applicable at large ranges (compared to the wavelength) from the source:

$$r^* \gg \lambda_0. \tag{21}$$

The inequality

$$|\eta_0| \ll \lambda$$

is the linearity criterion.

If $\lambda \leqslant \pi l$ then the linear solution (16) is valid when the condition

$$r^* \gg \frac{\lambda_0 R^2}{e(\pi l)^2}\frac{\sqrt{a^2+R^2}}{a}\left|\sin\left(\frac{Na}{U}\sin\varphi\cos\theta\right)\right| \tag{22}$$

is satisfied, which is equivalent for $Fr_a \leqslant 1$ to

$$r^* \gg \frac{\lambda_0 R^2}{e(\pi l)^2}\frac{\sqrt{a^2+R^2}}{a},$$

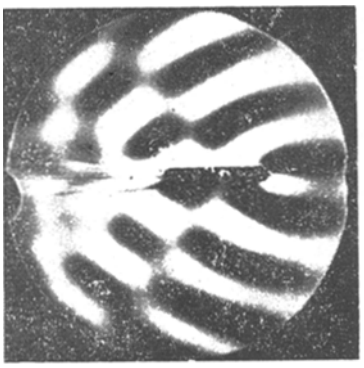

Fig. 1

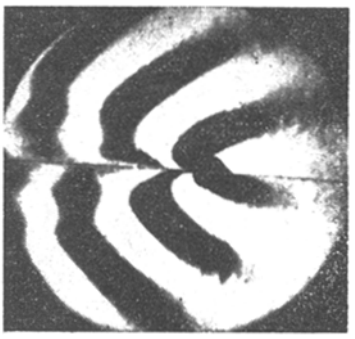

Fig. 2

and for $Fr_a \gg 1$ to

$$r^* \gg \frac{2R^2\sqrt{a^2+R^2}}{e\pi l^2}\,|\sin\varphi\cos\theta|,$$

where e is the base of the natural logarithms.

If $\lambda > \pi l$, then the linear solution (16) is valid when the inequality

$$r^* \gg \frac{R^2\lambda_0}{\lambda^2}\,\frac{\sqrt{a^2+R^2}}{a}\left|\sin\left(\frac{Na}{U}\sin\varphi\cos\theta\right)\right| \tag{23}$$

is satisfied, which is equivalent for $Fr_a \leqslant 1$ to

$$r^* \gg \frac{R^2\lambda_0}{\lambda^2}\,\frac{\sqrt{a^2+R^2}}{a},$$

and for $Fr_a \gg 1$ to

$$r^* \gg \frac{2\pi R^2\sqrt{a^2+R^2}}{\lambda^2}\,|\sin\varphi\cos\theta|.$$

It follows from (22) and (23) that a domain exists near the X axis where the linear solution is not valid.

An experimental investigation of apparent internal waves was performed in a 1.5 × 0.4 × 0.4 m laboratory tank filled with an aqueous solution of common salt with a homogeneous concentration gradient (density), $\Lambda = 4.4$ m, $N = 1.5$ sec^{-1}, $T = 4.2$ sec. The phase patterns were recorded by using an IAB-451 shadowgraph, and the amplitudes by using a "single-point" contact converter of the electrical conductivity [11]. The boundaries of the dark and light bands on the shadow photograms are the peaks and valleys of the waves; the blackening density is proportional to the wave amplitude. The tests performed showed that because of the blocking effect in the stratified fluid, the fluid velocity and density profiles vary at ranges on the order of a diameter ahead of and behind the body. It can hence be considered that internal waves are radiated by the whole system consisting of the body and the fluid it entrained. In connection with the presence of viscosity, the entrained fluid has an ovoidal shape.

The wave pattern in the XZ plane that occurs during horizontal motion of an elongated body d = 1 cm, L = 8 cm with velocity U = 1 cm/sec, T = 4.2 sec is represented in Fig. 1. The break in the wave surfaces observed in the moving picture presented is explained by a phase jump of π as the sign of $\sin((Na/U)\cos\theta)$ changes. The angles θ_p at which the break occurs are determined from the condition

$$(Na/U)|\cos\theta_p| = \pi p,\quad p = 1,2,3,\ldots \tag{24}$$

In this case ($\theta_p = 56°$, p = 1), it follows from (24) that $2a = 7.6$ cm, which agrees approximately with L.

Because of the blocking effect, an analogous pattern can be observed in the motion of a sphere (Fig. 2, y = 0, d = 2 cm, U = 1.02 cm/sec, T = 4.2 sec, Fr = 0.11, $\theta_1 = 20°$). Here $a = 2.25$ cm is determined from (24).

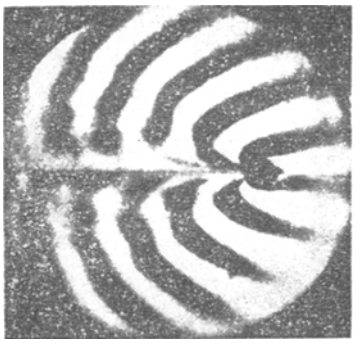

Fig. 3

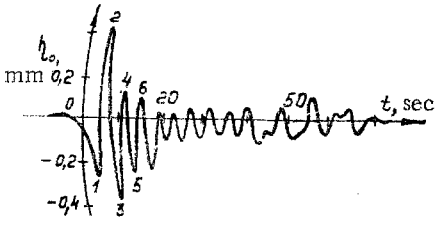

Fig. 4

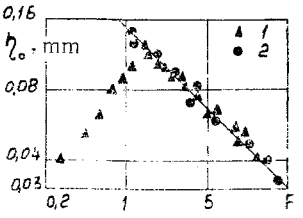

Fig. 5

The wave pattern in the XZ plane that occurs during horizontal motion of a sphere d = 2 cm with velocity U = 0.64 cm/sec, T = 4.2 sec, Fr = 0.044 is represented in Fig. 3. As the velocity diminishes, the effective horizontal dimension of the domain of internal wave excitation increases. A break in the phase surface is observed on the shadowgram at the angle $\theta_p = 39°$ (p = 2) and in the interference maximum of the amplitude at the angle $\theta_n = 22°$ (n = 2) to the motion axis. Substitution of the mentioned values of θ_n and θ_p in (18) and (24) yields similar values for the half-range between the centers of the sources $a_1 = 3.6$ cm and $a_2 = 3.45$ cm.

The solutions (13), (14), (16) obtained are antisymmetric with respect to the plane (line) z = 0 in the three-dimensional (planar) case. Mathematically this is associated with the change in sign of sin φ or (z) during passage from the upper to the lower half-space (half-plane), and physically with the opposite initial displacements in these half-spaces (half-planes). It is seen in Figs. 1-3 that the wave crest in the upper half-plane corresponds to the trough in the lower.

A recording of measurements of the magnitude of the vertical fluid particle displacement η(0, y, z, t) is presented in Fig. 4 for horizontal motion of the sphere d = 2.5 cm with velocity U = 1.65 cm/sec, T = 4.2 sec, Fr = 0.19 at the point y = 0, z = 5 cm. The points 1, 3, 5 are the troughs, and 2, 4, 5 the crests. The arrival time computed by means of (16) for the wave crests and troughs at the measurement points t_n = 2.9, 5.5, 7.8, 10, 12.1, 14.2 sec (n = 1, 2, ..., 6) is in good agreement with those observed experimentally even for the primary waves. For the case given the solution (16) agrees with experiment for the selection $a = 2.5$ cm, $l \simeq 1$ cm; then the computed ratios of the vibration spans $\frac{|\eta_0|_{n+2} + |\eta_0|_{n+1}}{|\eta_0|_{n+1} + |\eta_0|_n}$ (n = 1, 2, 3, 4) equal 1.4, 1.38, 1.25, 1.2. It follows from the recordings that these ratios are 0.88, 1.56, 1.24, 1.14. As the range to the source increases, the difference between the computed and observed quantities diminishes.

The dependence of the maximum particle displacement in the internal wave is represented in Fig. 5 for horizontal motion of a sphere of diameter d = 1 cm in a fluid with Λ = 4.2 m (point 1) and Λ = 17 m (point 2) at the point y = 0, z = 12 cm. The slope of the line on the graph corresponds to the dependence $Fr^{-1/2}$ which agrees with the law for the decrease in the amplitude $\eta_0 \sim 1/U$ for Fr ≫ 1, while $l \simeq 1.3$ cm for Fr < 0.8.

As the sphere moves with high velocities (Fr > 1) $l < d/4$, and $a < d$ also diminishes as the velocity increases.

The solution (16) obtained agrees satisfactorily with laboratory test results even at distances on the order of $2\lambda_0$.

Since the wavelength is less or on the order of the body dimensions for Fr $\ll$ 1, then the influence of viscosity should be taken into account in determining the amplitude characteristics of the internal waves.

LITERATURE CITED

1. M. J. Lighthill, "Studies on magnetohydrodynamic waves and other anisotropic wave motions," Philos. Trans. R. Soc. London, 252A, No. 1014 (1960).
2. M. J. Lighthill, "On waves generated in dispersive systems by traveling forcing effects, with applications to the dynamics of rotating fluids," J. Fluid Mech., 27, Pt. 4 (1967).
3. K. S. Peat and T. N. Stevenson, "Internal waves around a body moving in a compressible density-stratified fluid," J. Fluid Mech., 70, Pt. 4 (1975).
4. T. Y.-T. Wu and C. C. Mei, "Two-dimensional gravity waves in a stratified ocean," Phys. Fluids, 10, No. 3 (1967).
5. C. C. Mei, "Surface wave pattern due to a submerged source traveling in a stratified ocean," Report Hydrodynam. Lab. Mass. Inst. Technol., No. 92 (1966).
6. I. V. Sturova, "Wave motions occurring in a stratified liquid during flow around a submerged body," Prikl. Mekh. Tekh. Fiz., No. 6 (1974).
7. J. W. Miles, "Internal waves generated by a horizontally moving source," Geophys. Fluid Dynam., 2 (1971).
8. V. P. Dokuchaev and I. S. Dolina, "Radiation of internal waves by sources in an exponentially stratified fluid," Izv. Akad. Nauk SSSR, Fiz. Atmos. Okeana, 13, No. 6 (1977).
9. N. E. Kochin, I. A. Kibel', and N. V. Roze, Theoretical Hydromechanics [in Russian], Pt. 1, GIFML, Moscow (1963).
10. V. N. Nekrasov, A. M. Trokhan, and Yu. D. Chashechkin, "Internal wave generation in a plane laminar medium by uniformly moving hydrodynamic source (three-dimensional problem)," Brief Texts of Reports to Seventh All-Union Symposium on Wave Diffraction and Propagation [in Russian], Vol. 3, Moscow (1977).
11. V. I. Levtsov and Yu. D. Chashechkin, "Highly responsive converter of fluid electrical conductivity," Abstracts of Reports to the Fourth All-Union Conf. "Metrology and Radio Electronics" [in Russian], VNIIFTRI, Moscow (1978).